BNL-NCS-29035
CONF-800979--16

NEW ASPECTS IN THE EVALUATION OF THERMAL NEUTRON CROSS SECTIONS*

S. F. Mughabghab

Brookhaven National Laboratory
Upton, N. Y. 11973, U.S.A.

An invited paper presented at the Conference On Nuclear Data Evaluation Methods And Procedures held at Brookhaven National Laboratory, September 22-25, 1980.

NEW ASPECTS IN THE EVALUATION OF THERMAL NEUTRON CROSS SECTIONS*

S. F. Mughabghab

Brookhaven National Laboratory
Upton, N. Y. 11973, U.S.A.

ABSTRACT

Because of recent advances in experimental techniques, which improved the accuracies of thermal capture and scattering cross sections by an order of magnitude, a more stringent approach in the evaluation of the thermal constants is developed. In the present approach, the following aspects are introduced: (1) a consistency between thermal cross sections, coherent and incoherent scattering lengths, and neutron resonance parameters is achieved; (2) a consistency between the isotopic and element cross sections is sought; in addition, for each isotope, the requirement that the partial cross sections add up to the total is fulfilled; (3) where possible, charged particle data particularly derived from (d,p) reactions on light and medium weight istopes are used in locating the positions and strengths of bound levels. Such a procedure is useful in the evaluation of the shape of the cross sections in the thermal region; and (4) the Lane-Lynn theory of direct capture is called upon to calculate thermal cross sections and check for consistencies for certain isotopes.

Extensive examples to illustrate these procedures are presented.

---

*This work was performed under the auspices of the U.S. Department of Energy.

I. INTRODUCTION

I would like to start this review by asking a question: Why study and evaluate thermal neutron cross sections?

The answer to this is that the neutron has a "charm" and the neutron interaction at thermal energies is fundamental and important for several reasons:

1. Thermal cross sections are fundamental in testing high energy theories. Examples which can be cited are the pion exchange[1-2] and the quark models[3]. The pion exchange model was called upon by Riska and Brown[1] to explain a 10% discrepancy between the measured cross section of H and previous calculations and by Hadjimichael[2] to calculate the radiative neutron-deuteron capture cross section (520 ± 50 μb). The quark model was applied by Carlitz et al.[3] to achieve consistency between measured and calculated neutron-electron interaction scattering length. The latter calculation gives an indication of the structure and charge properties of the neutron.

2. Thermal cross sections are important ingredients in low energy nuclear theory:

a. Accurate knowledge of the singlet and triplet scattering lengths of H is basic for theoretical models dealing with the (n,p) interaction.

b. Scattering lengths of the four nucleon systems, n-^{3}H and n-^{3}He, can also shed light on the nucleon-nucleon interaction.[4] Experimental values of the thermal neutron scattering lengths of ^{3}H and ^{3}He favor the Yukawa over the exponential form factors.

c. Spin dependent scattering lengths (and subsequently incoherent scattering lengths) of light and medium weight nuclides can test the accuracy of shell model calculations.[5]

3. Thermal total and partial capture cross sections provide experimental tests of the validity of the Lane-Lynn theory of direct capture. Verification of this theory will be presented. This will be followed by a discussion of the applicability and limitations of the theory.

4. For light and medium weight nuclides, thermal cross sections can compliment charged particle data in predicting spins and (d,p) spectroscopic factors of final states.

5. Thermal cross sections can check the completeness of resonance parameters and can be used to derive the potential scattering radius R which is important in optical model calculations.

6. Thermal cross sections are important in determining the absolute neutron capture γ-ray intensities which in turn are used as a tool in the identification of elements and impurities in samples.

7. Improved knowledge of the thermal cross sections are required for reactor cycle and burn-up calulations. This would result in improved design of thermal reactors.

8. Thermal cross sections are used as standards. Examples are the capture cross sections of ^{197}Au, ^{59}Co, ^{55}Mn, the scattering cross sections of H, C, Si, V, Ni, and the fission cross sections of ^{235}U, ^{239}Pu.

II. PROCEDURE IN THE EVALUATION

We briefly outline in this section the various steps involved in the evaluation of thermal cross sections.

1. The first step in any evaluation is compilation of the experimental data. A complete and correct documented data base must be available. The CSISRS Library can be used for that purpose with a supplementation of the most recent data which may not be yet in the computerized files.

2. This is followed by a reduction of the data to a standard form. The following steps are required:

a. The reported cross sections are normalized to the standard cross sections of ^{55}Mn, ^{59}Co, ^{197}Au, (capture), C, Si, V, Ni (scattering), ^{235}U, ^{239}Pu, ^{252}Cf (fission), and to the most recent recommend half lives and abundances.

b. Corrections for reactor neutron spectrum and isotopic impurities, if possible, are made. This can be achieved with the aid of catalogues of strong γ-ray intensities and resonances, provided that the authors reported the required information.

c. A correction due to the shape of the cross section is made. This is possible if the locations of positive energy resonances and bound levels are known.

3. Weighted averages of the normalized data are produced and internal and external errors are calculated.

4. The last step requires consistency checks.

a. A consistency between thermal capture cross sections, coherent and incoherent scattering lengths, and neutron resonance parameters is achieved.

b. A consistency between the isotopic and element cross sections is sought; in addition, for each isotope, the requirement that the partial cross sections add up to the total is fulfilled.

c. The Lane-Lynn theory of direct capture is called upon to calculate thermal cross sections and check for consistencies between thermal capture cross sections and scattering lengths for certain isotopes.

d. For light nuclides, one can utilize the principle of charge symmetry to calculate, for example, scattering cross sections. An excellent example is provided by the analysis of Hale and Dodder[6] for the reaction $p+^{3}He \Longleftrightarrow n+T$. These authors predicted the singlet and triplet scattering lengths $a_+=3.32$ fm, $a_-=4.45$ fm and consequently $a=3.6$ fm.

5. In the actinide region, one can achieve additional consistency between σ_γ, σ_f, σ_a, σ_s, $\alpha,\eta,\bar{\nu}$ by the least squares method.

Since this method is adequately described by Leonard[7] and Lemmel[8] I will forego its discussion.

III. THEORETICAL CONSIDERATIONS

At this stage, it is important to review some of the theoretical relations which will be used extensively in the discussion.

A. Coherent Scattering Amplitudes

The spin dependent scattering amplitudes a_+ and a_- associated with s-wave resonances of spins I + 1/2 and I - 1/2 (where I is the spin of a target nucleus) can be written in terms of the resonance parameters as

$$a_{\pm} = R' + \sum_j \frac{\lambda_j \Gamma_{nj}}{2(E-E_j)-i\Gamma_j} \qquad (1)$$

where the summation is carried out over resonances with the same spin. The total coherent scattering amplitude is then the sum of the partial amplitudes weighted by their spin statistical factors g_+ and g_-,

$$a = g_+ a_+ + g_- a_-$$

$$g_+ = \frac{I+1}{2I+1} \qquad g_- = \frac{I}{2I+1} \qquad (2)$$

The coherent scattering amplitude for each spin state Eq. (1) can be separated into real and imaginary parts:

$$a_{coh} = R' + \sum_j \frac{\lambda_j \Gamma_{nj} (E-E_j)}{4(E-E_j)^2+\Gamma_j^2} + i \sum_j \frac{\lambda_j \Gamma_{nj} \Gamma_j}{4(E-E_j)^2+\Gamma_j^2} \qquad (3)$$

$$= a_r + i a_i$$

where a_r and a_i are the real and imaginary components, respectively. It is interesting to note that the imaginary part can be related to the absorption cross, σ_a by:

$$a_i = \frac{k \sigma_a}{4\Pi} \qquad (4)$$

where k is the wave number.

With the exception of few nuclides, neutron resonances are located far away from thermal energies. Under these conditions and for $E_j \gg \Gamma_j$ the coherent scattering amplitude takes the simple form

$$a = R' - 2.277 \times 10^3 \frac{r^0_{nj}}{E_{oj}} \quad . \qquad (5)$$

Another important relation which is required in the analysis of experimental data is the one between the free, a, and bound, b, coherent scattering amplitudes

$$b = \left(\frac{A + 1.0087}{A} \right) a + Z\, b_{ne} \qquad (6)$$

where b_{ne} is the neutron-electron interaction length. Its most accurate value was determined recently by Koester et al.[9]

$$b_{ne} = -\left(1.38 \pm 0.03\right) \times 10^{-3} \text{ fm} \quad .$$

The coherent and spin-incoherent free scattering cross sections can be described in terms of the coherent scattering amplitudes by:

$$\sigma_{coh} = 4\Pi \left(g_+ a_+ + g_- a_-\right)^2$$

$$\sigma_{inc\ (spin)} = 4\Pi\, g_+ g_- \left(a_+ - a_-\right)^2 \quad . \qquad (7)$$

For an element with several isotopes, an additional incoherent scattering cross section arises due to differences in the coherent scattering amplitudes of the various isotopes.

$$\sigma_{inc\ (isotopic)} = 4\pi \sum_m \sum_n \frac{1}{2} f_m f_n (a_m - a_n)^2 \qquad (8)$$

where f_n and a_n are respectively the abundance and the scattering amplitude of the n-th isotope.

In recent years, specialized techniques based on the wave properties of the neutron (interference, refraction, reflection, and diffraction) have been developed which resulted in highly improved knowledge of the coherent scattering amplitudes of the various isotopes and elements. These methods, as well as the Christiansen filter method, are described in the excellent review article by Koester.[10]

These relations provide the link between the thermal neutron cross sections and resonance parameters and can serve to check the consistency of the resonance parameters. A knowledge of the magnitude of the potential scattering radius R' at low neutron energies and its variation with mass number is required. This is derived from an analysis in the resonance region supplemented by theoretical calculations.[11] The variation of the potential scattering radius with mass number and its comparison with optical model calculations[11] is shown in Fig. 1.

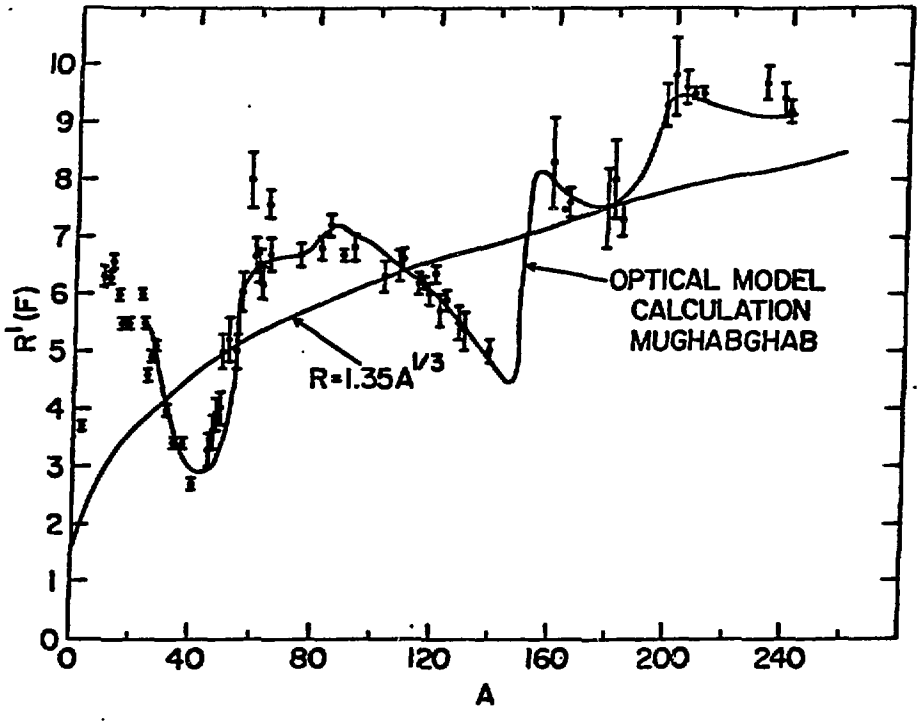

Fig. 1 A plot of the potential scattering radius with mass number, A.

B. Relationship Between S_{dp} and Γ_n^0

In this section, we present a useful relationship between the reduced neutron width Γ_n^0 and the (d,p) spectroscopic factor and determine the normalizing factor. In particular, the single particle dimensionless bound reduced neutron width for s-wave resonances is determined by a comparison of the experimental (d,p) and (n,n) data.

The (d,p) spectroscopic factor can be defined as the square of a ratio of dimensionless reduced neutron widths,

$$S_{dp} = \frac{\theta_n^2}{\theta_{sp}^2} \tag{9}$$

where θ_n^2 is expressed by:

$$\theta_n^2 = \frac{\gamma_n^2}{\frac{\hbar^2}{MR^2}} \tag{10}$$

and the reduced neutron width γ_n^2 for s-wave neutrons is defined as

$$\gamma_n^2 = \frac{\Gamma_n}{2kR} \tag{11}$$

where k is the wave number and R is the nuclear radius.

Substituting Eqs. (10) and (11) into (9), and using an interaction radius $R=1.35\ A^{1/3}$ fm, one gets

$$S_{dp} = 7.40\times10^{-5}\ A^{1/3}\ \frac{\Gamma_n^0}{\theta_{sp}^2} \tag{12}$$

where Γ_n^0 is expressed in eV units.

Note that θ_{sp}^2 is model dependent. For example the use of harmonic oscillator wave functions[12] gives $\theta_{sp}^2 = 0.036$. Instead of relying upon model calculations, we apply Eq. (12) to the $^{12}C+n$ system to derive θ_{sp}^2.

Meadows and Whalen[13] carried out a precise measurement of the total cross section of natural carbon (98.89% ^{12}C) in the energy region 100-1500 keV. Within the framework of single level R-matrix analysis, the authors obtained an excellent fit of the total cross section throughout the whole energy region. The derived reduced neutron width of the bound level at -2020 keV is γ_n^2 = 540 keV for an interaction radius of 4.80 fm. This bound level was studied by Darden et al.[14] by the (d,p) stripping reaction, for which a spectroscopic factor S_{dp} = 1.1 is obtained. Substituting these values in Eq. (12), one derives

$$\theta_{sp}^2 = 0.175$$

and hence,

$$S_{dp} = 4.21 \times 10^{-4} A^{1/3} \Gamma_n^0 \qquad (13)$$

This relation is used extensively in converting the (d,p) spectroscopic factors to reduced neutron widths.

C. The Lane-Lynn Theory of Direct Capture

Before recalling the essential relationships required in the analysis of partial and total capture cross sections, it is instructive to describe briefly the historical development of the experimental investigations dealing with this exciting field. Finally, the first quantitative verification of the Lane-Lynn[15] theory is presented.

1. Historical Pespective

a. In 1958, Groshev and his collaborators[16] observed a correspondence between γ- ray intensities and (d,p) spectroscopic factors for final states characterized by l_n=1 for the even-even target nuclides ^{24}Mg, ^{28}Si, ^{32}S, ^{40}Ca as well as odd even isotopes ^{23}Na, ^{27}Al, and ^{31}P. The suggestion was put forth[16] that a direct capture mechanism plays an important role in these nuclides.

b. Two years later, Lane and Lynn[15] formulated within the framework of R-Matrix theory a detailed theory of direct capture by subdividing phase space into internal and external regions. The partial capture cross sections for E1 transitions were explicitly calculated in terms of an algebraic expression. The essential feature of the theory is the dependence of the partial capture cross section on the (d,p) spectroscopic strength and on the gamma-ray energy.

c. The capture theory of Lane-Lynn motivated experimentalists[17] to search for a correlation between reduced γ-ray strengths, I_γ/E_γ^3, and stripping strengths, $(2J_f+1)\ S_{dp}$, where J_f is the spin of the final state populated by the γ-ray. For a quantitative study of the correspondence between (n,γ) and (d,p) data, Hughes, Kennett, and Prestwich[18] introduced the correlation coefficient:

$$\rho = \frac{\sum_i \left(\Gamma^0_{\gamma i} - \overline{\Gamma^0_\gamma}\right)\left(S_i - \overline{S}\right)}{\left[\sum_i \left(\Gamma^0_{\gamma i} - \overline{\Gamma^0_\gamma}\right)^2 \sum_i \left(S_i - \overline{S}\right)^2\right]^{1/2}} \qquad (14)$$

where $\overline{\Gamma^0_\gamma}$ and $\overline{S}$ are the average values and the summation is carried out over i=n final states. For the reaction $^{55}Mn(n,\gamma)\ ^{56}Mn$ a correlation coefficient ρ=0.84 for eight final states was found.[18] Similar studies were carried out for the Ca isotopes,[19-21] Ba, $^{138,142}Ce$, ^{142}Nd[22] which revealed in some nuclides high correlation coefficients approaching unity.

d. A significant development was the $^{37}Cl\ (n,\gamma)\ ^{38}Cl$ investigations of Spits and Akkermans[23] who reported at the Budapest Conference that the correlation coefficient was substantially improved when an E_γ instead of an E_γ energy dependence was considered. Other nuclides in the same mass region ^{27}Al, ^{31}P, ^{32}S, ^{40}Ar, and the Ca isotopes, exhibited the same trends.

e. Since such E_γ-dependence was not yet understood,[24] Kopecky, Lane, and Spits[25] pointed out that this behavior is predicted by the Lane-Lynn theory and arises because of the energy dependence of the radial dipole matrix element.

f. The observation[26] that high correlation coefficients were reported for those nuclides whose potential scattering radii, R', differ significantly from the interaction radius $R=1.35A^{1/3}$ indicated the presence of a (R-R') term in the direct capture cross section.

g. The previous observation motivated Mughabghab[27] to carry out the calculations in the framework of the Lane-Lynn theory and its verification for ^{136}Xe as well as ^{138}Ba, ^{144}Sm, and ^{29}Si was presented.[27]

2. The Direct Capture Cross Section for El Transitions. In this subsection, we present the expression for the direct capture cross section as derived by Lane and Lynn[15]:

$$\sigma_{\gamma f}^{(El)} = \frac{0.062}{R\sqrt{E'}}\left(\frac{Z}{A}\right)^2 \theta_{I_t}^2 \sum_{s'} \frac{(2J_f+1)}{6(2i_{s'}+1)} \frac{1}{|1-\rho' R_{s'}|^2} \times \left[y^2\left(\frac{y+3}{y+1}\right)^2 + 2\alpha'_{s'}\frac{y^2(y+2)(y+3)^2}{(y+1)^3} + (\alpha'^2_{s'}+\beta'^2_{s'})y^4\left(\frac{y+2}{y+1}\right)^2\right] \quad (15)$$

The reader is referred to the original article[15] for the nomenclature. In most cases, it can be shown that $B_{s'}$ which is related to the neutron capture cross section, is very small and as a result could be ignored in the relationship. For nonzero spin target nuclides ($I \neq 0$), s-wave capture results in channel spins $I+1/2$ and $I-1/2$. For equal capture in these components (i.e., A_s' is the same for the two channel spins) the above expression can be simplified to the following form:

$$\sigma_{\gamma f}(\text{potential}) = \sigma_{\gamma f}(\text{hard sphere})\left[1 + \frac{R-a_s}{R}\, y_f \frac{y_f+2}{y_f+3}\right]^2$$

$$\text{where } \sigma_{\gamma f}(\text{hard sphere}) = \frac{0.062}{R\sqrt{E_n}}\left(\frac{Z}{A}\right)^2 \mu \frac{2J_f+1}{6(2I_t+1)} S_{dp}\left(\frac{y_f+3}{y_f+1}\right)^2 y_f^2 \quad (16)$$

$$y_f^2 = R^2\, 2\, m\, E_\gamma / \hbar^2$$

and a_s is the coherent scattering amplitude.

The variable μ takes into account the multiplicity due to the incident-neutron channel spin. For $I_t = 0$, $\mu = 1$. However, for a target nucleus with nonzero spin, I_t:

$$\mu = 1 \quad \text{for } J_f = I_t \pm 3/2$$

$$\mu = 2 \quad \text{for } J_f = I_t \pm 1/2$$

It is interesting to note that the second term within the brackets of Eq. (16) represents the resonance channel contribution and it has a large effect in those nuclides where R is much

different from R; i.e., in the neighborhood of A=35 and 138 (Fig. 1).

We emphasize that Eq. (16) holds under the following conditions:

a. even-even nuclides,

b. for nuclides with $I \neq 0$ and a_s is the same for $I+1/2$ and $I-1/2$,

c. if a_s is not the same for $I+1/2$ and $I-1/2$, Eq. (16) is still applicable for transitions to final states with $J_f = I \pm 3/2$; otherwise, Eq. (16) needs modifications requiring the $p_{1/2}$ and $p_{3/2}$ components of S_{dp} as well as spin statistical factors.

3. Verification of the Lane-Lynn Theory. The experimental test of the Lane-Lynn theory of direct capture of slow s-wave neutrons was provided by the reaction ^{136}Xe (n,γ) ^{137}Xe. Three facts[27] presented signatures that direct capture plays a dominant role in the reaction mechanism of this isotope. These are: (1) nearby s-wave neutron resonances are not known in ^{136}Xe, (2) the neutron capture cross section is small,[28] and (3) the correlation coefficient between γ-ray and (d,p) strengths is maximized to a value of 0.984 for an $E_\gamma^{1.2}$ dependence of the partial capture cross sections.

On the left-hand side of Fig. 2 is demonstrated the variation of the correlation coefficient with the power, n, of the gamma-ray energy. On the right-hand side is represented the

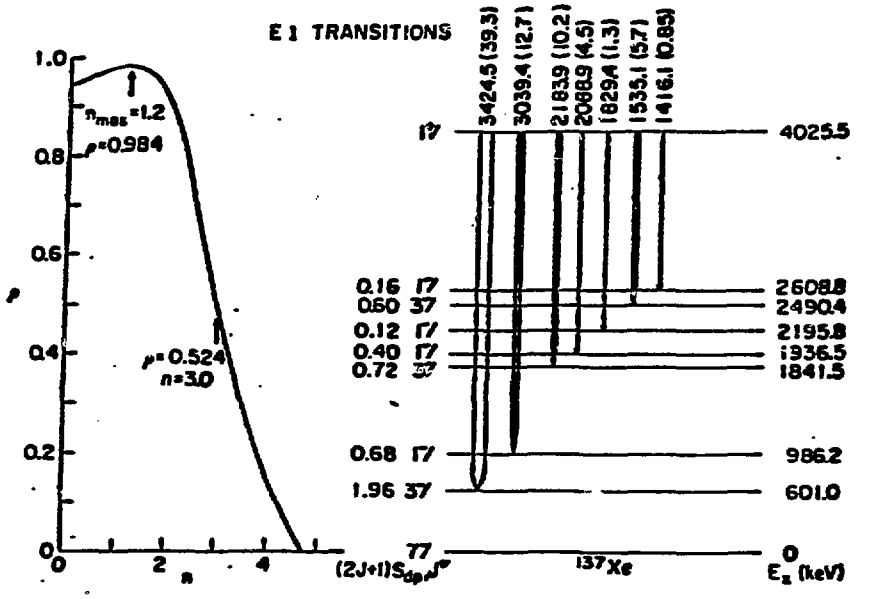

Fig. 2 Study of the variation of the correlation coefficient with the reduction factor n for the reaction ^{136}Xe$(n,\gamma)^{137}$Xe. Note that ρ approaches unity for n=1.2 which is a signature for direct capture. The right-hand side of the figure shows the measured primary E1 transitions populating the low lying states of ^{137}Xe.

pertinent E1 transitions feeding final states with large (d,p) strengths. The relative γ-ray intensities[29] are normalized to absolute values by two methods[27] which yield results accurate to within 10%. These are displayed in the second column of Table 1. The final states, their spins, and spectroscopic strengths are shown in columns 3, 4, 5, respectively. The partial capture cross sections are calculated with the aid of Eq. (16) based on the parameters of Table 1 and an interaction radius of $1.35\ A^{1/3}$ fm. The last column gives the experimental partial capture cross sections obtained by $\sigma_{\gamma f} = I_{\gamma f}\sigma_\gamma$ where $\sigma_\gamma = 260 \pm 20$mb. As shown, the agreement between the theoretical and experimental values is remarkable. Additional impressive examples are presented in Section IV.

Table 1

$^{136}Xe\ (n,\gamma)\ ^{137}Xe$

E_γ(keV)	$I_{\gamma f}$(%)	E_x(keV)	J_f	$(2J_{f+1})S_{dp}$	$\sigma_{\gamma f}$ (mb) Theo	$\sigma_{\gamma f}$ (mb) Exp.
3424.55	39.3±3.9	601	$^3/_2$	1.96	104	102
3039.37	12.7±1.7	986	$^1/_2$	0.68	30.6	33.3
2183.88	10.2±0.9	1841	$^3/_2$	0.72	23.9	26.5
2088.93	4.5±0.5	1936	$^1/_2$	0.40	12.7	11.7
1829.44	1.3±0.1	2106	$^1/_2$	0.12	3.3	3.4
1535.09	5.7±0.6	2490	$^3/_2$	0.60	14.1	14.8
1415.91	0.85±.09	3609	$^1/_2$	0.16	3.5	2.2
SUM	74.55			4.64	192.1	193.9

IV. APPLICATIONS

In this section, we present several interesting and remarkable examples illustrating the ideas and principles developed in the previous sections.

A. The Capture Cross Section and Absolute γ-ray Intensities of $^{12}C\ (n,\gamma)\ ^{13}C$.

The pertinent E1 transitions in the reaction $^{12}C\ (n,\gamma)\ ^{13}C$ are the ground state transition $s_{1/2} \longrightarrow p_{1/2}$ and the transition feeding the second excited state $s_{1/2} \longrightarrow p_{3/2}$. With the aid of

the (d,p) spectroscopic factors measured by Darden et al.[14] (H D optical model parameters) and an interaction radius $1.35A^{1/3}$ (3.09 fm), the partial capture cross sections are calculated by Mughabghab[31] for the first time and are presented in Fig. 3. A total capture cross section of 3.39 mb is then obtained, which is in good agreement with a recommended[28] value of 3.4±0.3 mb and with the most recent accurate value[32] 3.53±0.07 mb.

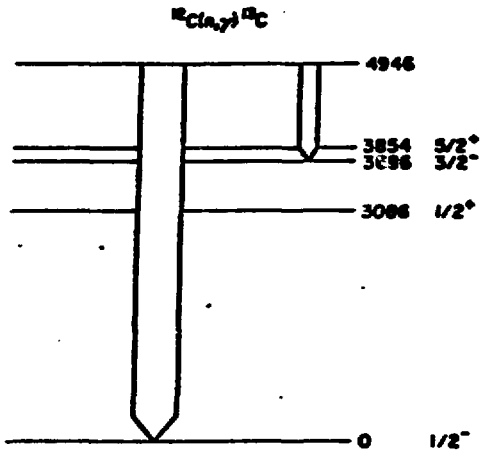

E_γ(keV)	(2J+1)S	I_γ(%) THEORY	I_γ(%) EXP.	σ_γ(mb) THEORY
4946	2.2	67.3	67.47±.92	2.28
1260	0.4	32.7	32.14±.64	1.11
				3.39

Fig. 3 Comparison between theoretical and measured partial capture cross sections as well as gamma-ray intensities for the reaction ^{12}C (n,γ) ^{13}C.

Included also in Fig. 3 are the measured[33] and calculated values of the two gamma-ray intensities. As indicated, the agreement between the two sets is indeed surprisingly remarkable in view of the fact that the spectroscopic factors are known to an accuracy of 10-15%. The other surprise which emerged from this study is the fact that the use of an interaction radius of $1.35\ A^{1/3}$ for a nucleus as light as ^{12}C described well the data. It is emphasized here that the same relationship for the interaction radius was used in the calculations of the radiative capture of neutrons by ^{136}Xe.

B. The Capture Cross Section of ^{13}C and the (d,p) Spectroscopic Factors

This nuclide provides us with an interesting example of interference phenomena between hard sphere and potential capture. As will be demonstrated shortly, a precise knowledge of the coherent scattering amplitude for channel spin I+1/2 is required. Since the spin of the target nucleus is 1/2, s-wave capture by ^{12}C results in spins of 1 and 0. The $p_{1/2}$ ground state and the second excited $p_{1/2}$ state at 6589 keV both have spins and parity 0^+ and therefore can be reached only by electric dipole radiation from capturing state 1^-. Therefore, the coherent scattering amplitude a_+ as well as the (d,p) spectroscopic factors must be known to a high degree of accuracy. At the start, let us check the consistency of the bound incoherent scattering amplitude, $b_+ - b_-$ with the (d,p) spectroscopic factors for s-wave states. Glattli et al.[34] employed the method of pseudomagnetism for measuring the spin dependent scattering amplitudes of slow neutrons for various isotopes. A value of $b_+ - b_- = -1.2 \pm 0.2$ fm was obtained.[34] Employing the Christiansen filter method, Koester et al.[35] obtained for ^{13}C, $b = 6.19 \pm 0.09$ fm. Combining these two measurements, one obtains:

$$a_+ = 5.47 \pm 0.09 \text{ fm}$$

$$a_- = 6.59 \pm 0.36 \text{ fm}$$

Table 2
Spectroscopic Information of ^{14}C

E_x (MeV)	E_n (MeV)	J^π	ℓ	S_{dp} (a)	θ^2 (b)	Γ_n^o (keV) (c)	S_{dp} (c)
0		0^+	1	2.61 2.09	0.067		
6.094	-2.083	1^-	0	0.87, 0.78	0.20	0.791	0.78
6.589		0^+	1		0.20		
6.903	-1.275	0^-	0	1.03	0.24	0.949	0.94

(a) Ref. 37 (b) ref. 36 (c) Present analysis

It is interesting to point out here that Normand[5] calculated within the framework of the shell model an incoherent scattering length $b_+ - b_- = -0.95$ fm for a value of $b = 6.19$ fm. This is in good agreement with a measured value of -1.2 ± 0.2 fm. Using

this latter value, the information[36] that the reduced neutron width of the state at 6.903 MeV is 1.2 times larger than that at 6.094 MeV, the contribution of positive energy resonances, and Eq. (5), one obtains reduced neutron widths 0.791 and 0.949 keV, respectively, for the 6.0944 and 6.903 MeV states of ^{14}C. These values correspond to spectroscopic factors Eq. (13) 0.78 and 0.94, respectively, and are included in Table 2. Note that the spectroscopic factor for the first excited state derived in this analysis is in excellent agreement with the value extracted by Datta[37] for the case where distorted wave Born calculations using optical model parameters of Watson[39] are applied. Because of this fact, a value of S_{dp}=2.09 instead of 2.61 for the ground state of ^{14}C is chosen in the calculation of the partial capture cross section feeding the ground state. The theoretical value for the ground state transition is found to be $\sigma_{\gamma 0}=1.19^{0.80}_{0.60}$ mb. The large errors on this value are a reflection of the uncertainty in $a_+(1.65\%)$! We emphasize that such large uncertainties in the calculated values are in general unusual. They are the exceptions rather than the rule. The ^{13}C nucleus represents a unique case of strong destructive interference between potential and hard sphere capture Eq.(16). This arises because of the comparatively large value of the γ-ray energy populating the ground state and the large negative difference between R and a_+, i.e., $R-a_+=-2.30$ fm. Because of this interesting situation, the variation of $\sigma_{\gamma 0}$ with a_+ is investigated and the results are described in Fig. 4. Of interest is the parabolically rapid change of $\sigma_{\gamma 0}$ with a_+. A minimum value occurs at about 5.2 fm and at 6.0 fm $\sigma_{\gamma 0}$ takes a value of 9 mb.

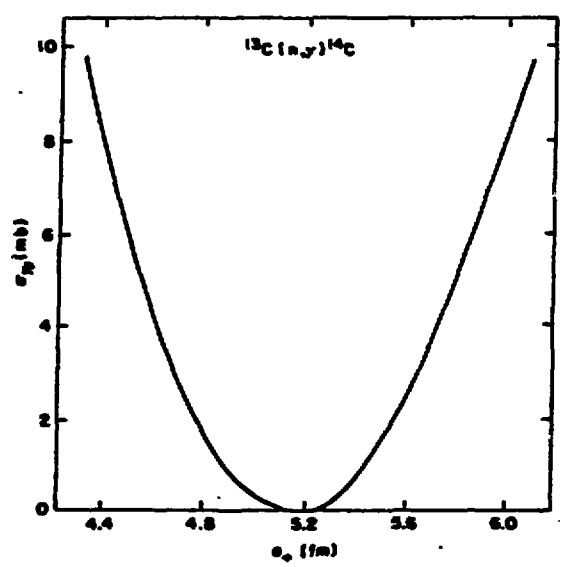

Fig. 4 Variation of the partial capture cross section populating the ground state of ^{14}C with the scattering length, a_+.

Comparison of the present calculations can be made with the very recent measurement of Lone[33] who determined the ^{14}C absolute gamma-ray intensities feeding the ground state and the second excited state at 6.589 MeV. These are (84.0±2.3)% and (8.5±0.5)%, respectively. In addition, the ratio of the capture cross sections of ^{13}C and ^{12}C was found to be:

$$\frac{\sigma_\gamma(^{13}C)}{\sigma_\gamma(^{12}C)} = 0.388 \pm 0.010 \quad .$$

Adopting a capture cross section[32] 3.53±0.07 mb for ^{12}C, one obtains σ_γ (^{13}C) =1.37±0.04 mb and a partial capture cross section 1.15±0.04 mb for the ground state transition. This value is in excellent agreement with the theoretical value 1.19 mb!

Since the spectroscopic factor for the 6.589 MeV state of ^{14}C is not yet determined, we apply Eq. (14) to obtain S_{dp}=0.058±0.004 for this state. It will be of interest to measure this value. A summary of the present results and measurement[33] is presented in Table 3.

Table 3
Comparison of Theoretical and Measured Partial Capture Cross Section for ^{13}C

E_γ (keV)	I_γ(%)	E_x(keV)	J^Π	ℓ	S_{dp}	σ_γ(mb)[b]	σ_γ(mb)[c]
8174	84.0±2.3	0	0^+	1	2.09[a]	1.10	1.15±0.4
1586	8.5±0.5	6589	0^+	1	0.058± 0.004 (b)		0.12± .01

(a) Ref. 37. Value corresponding to a Watson Potential
(b) Present Results
(c) Ref. 33

C. The Coherent Scattering Amplitudes of B, ^{10,11}B and the Capture Cross Section of ^{11}B

Because of interest by solid state physicists in the coherent and incoherent scattering amplitudes of natural boron and its stable isotopes, ^{10,11}B, we present in some detail an evaluation of these quantities and consequently apply the Lane-Lynn theory to obtain a better estimate of the capture cross section of ^{11}B. In addition, ^{11}B provides an interesting example of illustrating the requirement of modifying Eq. (16) in order to take into account the unequal contributions of the two channel spins of the initial state. At first, let us consider the coherent scattering amplitude of ^{11}B. Two discrepant values, one by Koester et al.[40] (b=6.66±0.02 fm) and the other by Craven and Sabine[41] (b=6.1±0.1 fm) are at present available. Recourse to the known positive[42] and negative[43] energy s-wave neutron resonances indicates that the resonance parameters, combined with a potential scattering radius of R =4.98 fm, are in agreement with b=6.66 fm. The former value is in excellent agreement with a potential scattering radius of $R' = R(1+\bar{R})$=4.95 fm derived from the data of White et al.[42] Furthermore, the resonance parameters provide information on the free spin-dependent scattering lengths:

$$a_+ = 5.27 \text{ fm}$$
$$a_- = 7.53 \text{ fm}$$

which yield an incoherent scattering amplitude $a_+ - a_- = -2.26$ fm and hence an incoherent scattering cross section of 0.150 b. We note here that, since the spin dependent scattering lengths have not yet been measured independently, it will be informative to determine them by the method of pseudomagnetism.[34] This is essential because of the important role of these quantities in the Lane-Lynn theory.

We draw attention to the point that a coherent scattering amplitude 6.66±0.02 fm for ^{11}B implies a vanishingly small value for the real part of the coherent scattering amplitude of ^{10}B (0.00±0.22 fm). This conclusion is based on b=5.34±0.04 fm for natural baron.[28] The imaginary component of ^{10}B coherent scattering amplitude can be determined with the aid of Eq. (4) and its value is 1.067±0.003 fm. A summary of the present analysis is shown in Table 4.

At this stage, let us turn our attention to the study of the ^{11}B capture cross section. Since the recommended[28] value, 5.5±3.3 mb, has such a large uncertainty, it is instructive to evaluate it in terms of the Lane-Lynn theory. However, because the scattering amplitudes for the two spin states of ^{11}B are quite different, the capture cross sections for the two channel spins $I \pm 1/2 = 2,1$ are different. As pointed out previously, the Lane-Lynn expression requires a modification to take into account the spin factors and the $p_{1/2}$ and $p_{3/2}$ amplitudes of the (d,p)

Table 4
Scattering Parameters of B and Its Isotopes

Abundance	B	^{10}B 19.8%	^{11}B 80.2%
b_r(fm)	5.34±0.04	0.00±0.22	6.66±0.02
b_i(fm)	0.2113±0.06	(1.067±.003)	
a_+(fm)		-3.21	5.27
a_-(fm)		4.03	7.53
R'(fm)		4.1	4.98
σ_s(b)	4.27±0.07	2.23±0.06	4.84±0.04
σ_{inc}(b)	1.26±0.03	2.11±0.08	0.15±0.03

spectroscopic factors of the final states.[44] Denote the $p_{1/2}$ and $p_{3/2}$ amplitudes of S_{dp} by $S_{3/2}$ and $S_{1/2}$ so that $S_{dp}=S^2_{3/2}+S^2_{1/2}$. A comparison of the (d,p) and (n,γ) strengths for a target nucleus with spin I=3/2 (i.e. ^{11}B) is shown in Table 5. Note that for final spin states I±3/2 (i.e. J_f=3,0) the (n,γ) strengths are still correlated with the (d,p) strengths. Also note that for equal contributions from the two channel spins, 2 and 1, the interference terms between $S_{3/2}$ and $S_{1/2}$ cancel out, and as a result the (n,γ) and (d,p) strengths are still correlated. However, for unequal contribution from channel spins 2 and 1, it is obvious that the (n,γ) strength is no longer necessarily correlated with the (d,p) spectroscopic factors. Consequently, the Lane-Lynn relationship requires correction factors which are derived[31] and are described in Table 5.

In order to be able to carry out the calculations, the relative strengths of the $p_{1/2}$ and $p_{3/2}$ amplitudes need to be known. In principle, such information can be derived from (d,p) experiments carried out with vector-polarized deuterons. However, this knowledge is scanty, and therefore, as an alternative, one has to resort to some guidance from theoretical investigations similar to that of Cohen and Kurath.[45]

The pertinent electric dipole transitions in ^{12}B are those populating the ground state (1^+), the first, and fourth excited states at 953 keV (2^+) and 2724 keV (0^+), respectively. It is assumed that the M1 transition feeding the 1674 keV state (2^-) is weak. In the (d,p) study of Monahan et al.,[43] it is suggested that the ground and the first excited states are characterized by pure $p_{1/2}$ orbitals while the state at 2724 keV is a pure $p_{3/2}$

state. These are to be compared with the predictions of Cohen and Kurath[45] who described the ground state as possessing 14% $p_{3/2}$ component while the first and fourth excited states are pure $p_{1/2}$.

Table 5
Comparison Between (d,p) and (n,γ) Strengths For Electric Dipole Radiation of Target Nucleus with Spin I=3/2

(d,p) Strength	J_f	(n,γ) Strength Channel Spin 2	(n,γ) Strength Channel Spin 1
$7\,S^2_{3/2}$	3	$7\,S^2_{3/2}$	0
$5(S^2_{3/2} + S^2_{1/2})$	2	$\frac{5}{2}(-S_{3/2} + S_{1/2})^2$	$\frac{5}{2}(S_{3/2} + S_{1/2})^2$
$3(S^2_{3/2} + S^2_{1/2})$	1	$\frac{1}{2}(S_{3/2} - \sqrt{5}\,S_{1/2})^2$	$\frac{1}{2}(\sqrt{5}\,S_{3/2} + S_{1/2})^2$
$S^2_{3/2}$	0		$S^2_{3/2}$

and $p_{3/2}$ states respectively. Accordingly, the calculations of partial capture cross sections and γ-ray intensities are calculated on the basis of both of these conclusions regarding the components of the ground state. The results which are displayed in Table 6 show the calculated total as well as partial capture cross sections which are in good agreement with the experimental value, 5.5±3.5 mb. Also shown are the predictions of the absolute γ-ray intensities which have not yet been measured. In order to test these theoretical results, it will be of great interest to measure the total capture cross section with better accuracy as well as the gamma-ray spectra due to capture in ^{11}B.

Table 6
Theoretical Values of the Total, Partial Capture Cross Sections, and Absolute Gamma-Ray Intensities of ^{11}B

E_γ(MeV)	E_x(MeV)	J	S_{dp}[a]	σ_γ(mb)[b]	I_γ(%)[b]	σ_γ(mb)[c]	I_γ(%)[c]
3.370	0	1^+	0.69	3.77	58.9	3.54	57.4
2.417	0.953	2^+	0.55	2.56	40.0	2.56	41.5
0.646	2.724	0^+	0.21	0.07	1.1	0.07	1.1
Total				6.40	100	6.17	100

(a) Ref. 43
(b) Present results on basis of a pure $p_{1/2}$ ground state
(c) Present results on basis that the ground state contains 14% $p_{3/2}$ component.

D. Neutron and Nuclear Spectroscopy of ^{19}F

So far, we have dealt with the evaluation of thermal cross sections. Now, we present an example illustrating the inverse process whereby the thermal constants can be used as a powerful tool in the evaluation of the s-wave resonance parameters and the deduction of properties of bound p-states. This can best be appreciated by examining the $^{19}F(n,\gamma)^{20}F$ and $^{19}F(n,n)^{19}F$ reactions at thermal energies. Fluorine is especially important in view of its possible use in the design of the breeder blanket for fusion reactors.

The total neutron cross section of ^{19}F ($I^\pi = 1/2^+$) reveals[46] an unresolved doublet at 270 keV, one component of which is an s-wave resonance whose parameters are naturally not well determined[28] (Γ = 25±10 keV, Γ_γ = 4.2±1.8 eV). The negative sign of the incoherent scattering amplitude[47] ($b_+ - b_-$ = -0.19±0.02 fm) can be accounted for in terms of either a bound s-wave resonance with zero spin or alternatively a positive resonance with spin 1. The polarization data of Gul'ko et al.,[48] which indicate that 42% to 70% of the capture of thermal neutrons is formed in channel spin 1, is the arbitrator, thus confirming a spin assignment of 1 for the 270 keV resonance. In fact, it will be shown shortly that 75% of thermal capture takes place in channel spin 1. Attributing the difference in the

coherent scattering amplitudes, b_+ and b_-, to the s-wave 270 keV resonance, and applying Eq. (5), one derives a value, Γ_n =11±1 keV. The error is attributed to the uncertainty of the incoherent scattering amplitude. The present value of the neutron scattering width is in reasonable agreement with the previous estimate.[28]

To determine the radiative width of the 270 keV resonance, the direct capture cross section have to be determined. This is achieved by describing the two transitions populating the ℓ_n=1 final states to a direct capture mechanism. On the basis of this assumption, which will be subsequently verified, a value of 4.7 mb is obtained on the basis of a total capture cross, 9.6±0.5 mb, and the known E1 gamma-ray intensities.[49]

The difference between these values, (9.6-4.7=4.9 mb) is attributed to internal resonance capture arising from the s-wave resonance at 270 keV. With the aid of the Breit-Wigner relationship, one obtains then a radiative width of 4.9±0.7 eV for the 270 keV resonance.

Because the coherent scattering amplitudes of the two channel spins are practically the same, it follows then that the direct capture components of the corresponding channel spins are equal. Therefore, the total capture cross section in channel spin 1 is equal to 7.25 mb (4.9+4.7x1/2). Consequently, 75% of the capture is formed in channel spin 1. This is in conformity with the upper limit reported by Gul'ko et al.[48]

The (d,p) spectroscopic factors and spins of the ^{20}F states at E_x=5937 keV and 6019 keV can be determined by applying Eq. (16) and the information[50] that the (d,p) cross section of the 6019 keV state is about 1.5 times that of the 5937 keV state. The absolute intensities of the gamma rays feeding these two states were adopted from the investigations of Spilling et al.[49] because of the use of a filtered thermal beam to remove the contribution of fast neutrons. The results of the present analysis are displayed and are compared with those of Mosley and Fortune.[51] As shown, the agreement in the values of the spectroscopic factors is indeed very good. However, there is a marked discrepancy with regard to the spin assignment of the 6019 keV state. The present study indicates that μ=2 and hence J=1 for this state. One plausible explanation of the discrepancy is the postulation that the 6019 keV state is a closely spaced doublet, one component of which is characterized by ℓ_n=3, $J=2^-$.

On the other hand, combining the present results with those of Ajzenberg-Selove,[52] ($J^{\pi}=1^-,2^-$) one arrives at a spin assignment of $J^{\pi}=2^-$ for the 5937 keV state.

Table 7
Nuclear Spectroscopy of ^{20}F P-States

E_γ(keV)	I_γ(%) (a)	$\overline{\mu}$	σ_γ(mb) (b)	E_x(keV)	S_{dp} (c)	S_{dp} (d)	J^π (c)	J^π (d)
665.5	15.4	1	1.46	5937	0.588	0.43	$2^-, 0^-$	
583.5	34.0	2	3.23	6019	0.714	0.68	1^-	2^-

(a) Ref. 50
(b) Experimental partial capture cross sections
(c) Present study
(d) Ref. 51

E. The Direct Capture Components of $^{20,22}Ne$, ^{26}Mg, and ^{34}S

For many of the light to medium weight nuclides, the number of final states which are characterized by a neutron orbital angular momentum, ℓ_n=1, is limited. As a consequence, this aspect renders the study of the reaction mechanism with the aid of correlation analysis limited.[53] This difficulty now is resolved, thanks to the ^{136}Xe (n,γ) ^{137}Xe reaction,[27] by carrying out the quantitative calculations, Eq. (16), and subsequently making a comparison with the experimental data. In this section, we present $^{20,22}Ne$, ^{26}Mg, and ^{34}S as representative examples illustrating this situation. The absolute gamma-ray intensities and (d,p) spectroscopic factors are surveyed and collected from the literature and compilations.[54] The calculations of partial capture cross sections are carried out by the author adopting the procedures described previously. The results are displayed in Table 8. As is readily evident by inspection of the last two columns, there is a general good agreement between the theoretical and experimental values. It seems that the theory can predict the strong transitions to an accuracy ranging from 6% to 15% as opposed to 30% for the weaker ones. This trend can be attributed to the uncertainty in both the spectroscopic factors and the γ-ray intensities. However, there is a marked discrepancy for the 2083 keV gamma line of ^{35}S. As noted in Table 8, the calculated value is 25.9 mb compared to a measured value of 41.4 mb. An internal resonance capture component of 1.9 mb, which is interfering constructively with the direct capture component and is due to the s-wave resonances at

301 and 357 keV, can resolve this discrepancy. This is achieved if a radiative width of about 2 eV is attributed to these resonances.

Table 8
Theoretical and Experimental Partial Capture Cross Sections of $^{20,22}Ne$, ^{26}Mg, ^{34}S

Isotope	E_γ (MeV)	$I_\gamma Z$	$(2J_f+1)S_{dp}$	σ_γ (mb) (a)	σ_γ (mb) (b)
^{20}Ne	2.536	80.7	2.4	29.9	29.8
^{20}Ne	1.070	13.6	0.48	5.0	4.4
^{22}Ne	1.980	75.0	1.2	26.2	22.5
^{22}Ne	1.364	12.5	0.22	4.5	3.0
^{26}Mg	2.882	62.0	1.6	23.7	21.1
^{26}Mg	1.615	11.7	0.62	4.5	6.5
^{34}S	4.638	56 ± 6	2.1	128.8	120
"	3.184	7.0 ± 0.9	0.4	16.1	15.2
"	2.797	6.1 ± 0.8	0.3	14.0	11.0
"	2.083	18 ± 1.5	0.96	41.4	25.9
"	2.023	12 ± 1.5	0.76	27.6	21.0

(a) Experimental Values
(b) Present Study

F. The Thermal Constants of the Ca Isotopes

As was pointed out previously, the Ca isotopes were among the first to reveal large correlation coefficients between reduced gamma-ray intensities and (d,p) spectroscopic strengths, [19-20]

thus suggesting that direct capture plays an important role in the reaction mechanism. Because of historical reasons as indicated earlier, it is instructive to carry out the numerical calculations of the capture cross sections for the purpose of comparing the results with the corresponding measurements. In addition, as was stressed previously in the many examples we explored, this procedure allows the determination of the coherent scattering lengths as well as the evaluation of the thermal cross sections. However, an apriori knowledge that direct capture dominates is required. Because of space limitations, the results are briefly described for each isotope.

1. $^{40}Ca\ (n,\gamma)\ ^{41}Ca$:

Although ^{40}Ca is a doubly magic nucleus with the expectation that the direct capture mechanism is totally dominant, a comparison between the theoretical and experimental partial capture cross sections indicates a lack of good general agreement. This is attributed to internal resonance capture (compound processes) resulting from capture in the tail of a nearby bound s-wave level. However, we note that the transition populating the excited state 1943 keV (S_{dp}=1.25) shows reasonable agreement, whereby the computed value is 119 mb as compared to an experimental value of 152 mb.

2. $^{42}Ca(n,\gamma)\ ^{43}Ca$:

This isotope exhibits a large correlation coefficient, 0.91, between reduced gamma-ray intensities and (d,p) strengths. However, since the coherent scattering length is not experimentally determined, the calculations cannot be carried out readily. Alternatively, we applied the measured partial capture cross section feeding the excited state at 2046 keV (E_γ=5886 keV) to arrive at a coherent scattering length of 3.15±0.20 fm for ^{42}Ca. Subsequently, it is shown that the total capture cross section, 680±70 mb, is totally due to direct capture.

3. $^{44}Ca(n,\gamma)\ ^{43}Ca$

Since the coherent scattering amplitude for ^{44}Ca is well determined,[28] b=1.8±0.1 fm, one fortunately can carry out the calculations readily without resort to the use of any adjustable parameters. A total direct capture cross section of 867 mb is then derived which is in excellent agreement with a measured value, 880±50 mb. A comparison between the theoretical and measured partial capture cross sections is described in Fig. 5 and detailed in Table 9. The (d,p) spectroscopic factors are adopted from Ref. 55. Note the remarkable agreement between theory and experiment, particularly for the two gamma-ray transitions feeding the excited states at 1435 and 1900 keV.

4.. $^{46}Ca(n,\gamma)\ ^{47}Ca$:

A coherent scattering amplitude, b=2.55±0.25 fm, is derived for this nucleus.

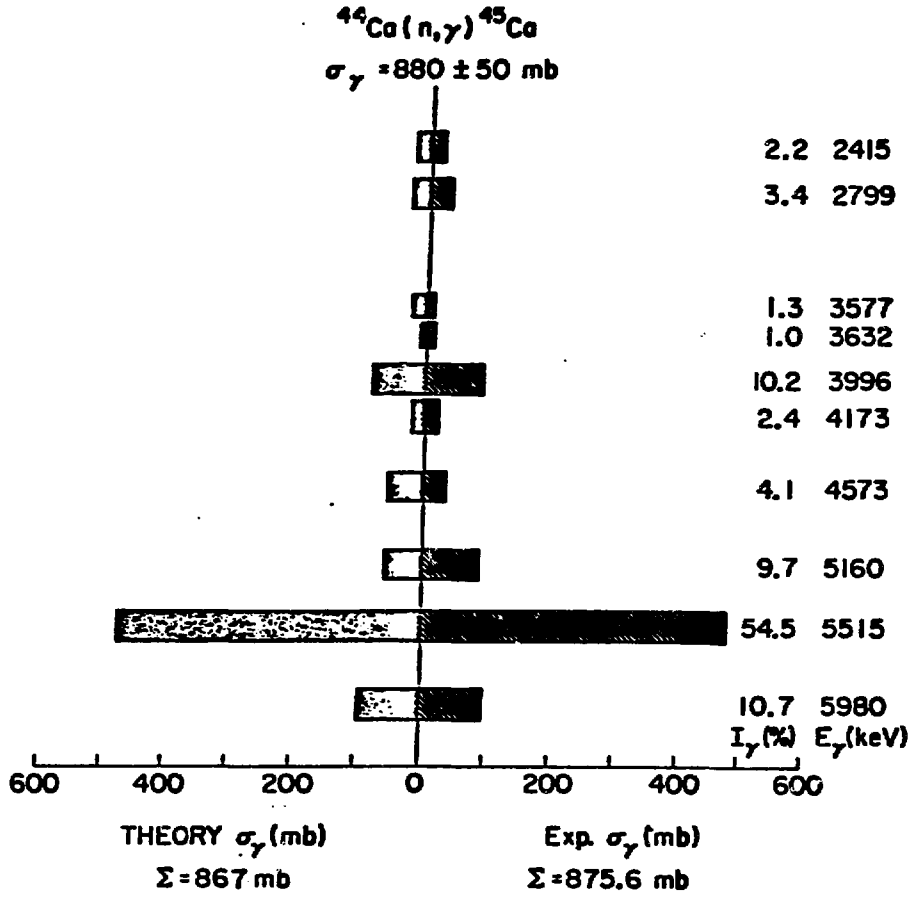

Fig. 5 Comparison of predicted and measured partial capture cross sections for the reaction $^{44}Ca(n,\gamma)\ ^{45}Ca$. The two columns on the right-hand side represent the absolute gamma-ray intensities and the corresponding γ-ray energies. A total capture cross section of 867 mb is predicted, which is in very good agreement with the experimental value, 880 ± 50 mb, thus demonstrating that direct capture dominates in this case.

Table 9
Theoretical and Experimental Comparisons
of Partial Radiative Widths for $^{44}Ca(n,\gamma)\ ^{45}Ca$

E_γ(keV)	E_x(keV)	$(2J_f+1)\ S_{dp}$ [a]	I_γ(%) [b]	σ_γ(mb) [c]	σ_γ (mb) [d]
5980.3	1435	0.40	10.7	94	96
5515.1	1900	2.20	54.5	480	475
5165.5	2249	0.30	9.7	85	59
4572.5	2842	0.34	4.1	36	57
4173.0	3242	0.14	2.4	21	21
3996.0	3419	0.49	10.2	90	69
3631.5	3783	0.08	1.0	9	10
3576.8	3838	0.19	1.3	11	23
2799.3	4616	0.34	3.4	30	30
2415.4	4999	0.36	2.2	19	27
SUM			99.5	875	867

a) Ref. 20
b) Ref. 55
c) Experimental values
d) Present theoretical calculations

5. $^{48}Ca(n,\gamma)\,^{49}Ca$:

Similarly, a coherent scattering amplitude, b=1.5±0.2 fm is calculated for ^{48}Ca. We point out here that, since this is significantly smaller than R =3.1 fm for A=48 (Fig. 1), this value suggests the presence of a positive energy s-wave resonance. It is interesting to search for this resonance by carrying out total cross section measurements below 30 keV, an as yet unexplored energy region.

G. Estimates of Capture Cross Sections of Fission Products

Finally, we note here that the procedures outlined previously can be applied to the estimations of capture cross sections of fission products. For example, in WRENDA 76/77 two requests for the thermal capture cross sections $^{132}Te(n,\gamma)\,^{133}Te$ and $^{126}Sn(n,\gamma).\,^{127}Sn$ are noted for the purpose of calculations of fission product poisons.

Since both of these nuclides are radioactive with comparatively short half lives, it is experimentally difficult, as yet, to determine the cross sections easily. This can be circumvented by carrying out the calculations in the framework of the Lane-Lynn theory on the simple assumption that the single particle (d,p) strengths in ^{126}Sn and ^{132}Te are the same as those in the corresponding stable isotopes, ^{124}Sn and ^{130}Te, for which $(2J_f+1)S_{dp}$ values are available. The results of these calculations[55] are:

$$^{126}Sn\ (n,\gamma)^{127}Sn \qquad \sigma_\gamma = 0.120b$$

$$^{132}Te\ (n,\gamma)^{133}Te \qquad \sigma_\gamma = 0.135b$$

We stress that if low-lying resonances are located close to thermal energies, which is most unlikely, then these values are considered as lower limits.

V. CONCLUSION

To summarize, we outlined briefly the various interesting reasons for the study of thermal cross sections, described a procedure in the evaluation, discussed the relations employed in the analysis, and placed emphasis on the Lane and Lynn theory of direct capture. In the third section, we explored the application of the Lane-Lynn theory to the light and medium weight isotopes and discovered remarkable agreement between theory and experiment, particularly for $^{12,13}C$ and ^{20}F, and some of the Ca isotopes. In additions, we were able to derive (d,p) spectroscopic factors, spins of final states, and scattering lengths. In some cases, we pointed out some fruitful ideas for future investigations.

Finally we emphasize that these methods and procedures are applied in the evaluation of the thermal cross sections and

resonance parameters which will appear in the forthcoming edition of BNL 325, Vol. 1.

Finally, I hope I was able to convey to you some of the excitement which can be derived in the study and evaluation of thermal cross sections.

VI. ACKNOWLEDGEMENT

The author is greatly indebted to Dr. M. A. Lone for sending his $^{12,13}C$ data prior to publication and to Professor L. Koester for a stimulating correspondence regarding the coherent scattering amplitudes of B and its isotopes.

VII. REFERENCES

1. D. O. Riska and G. E. Brown, Phys. Letters B38, 193 (1972).
2. E. Hadjimichael, Phys. Rev. Letters 31, 183 (1973).
3. R. D. Carlitz, S. D. Ellis, and R. Savit, Phys. Letter B 68, 443 (1977).
4. V. F. Kharchenko and V. P. Levashev, Nucl. Phys. A243, 249 (1980).
5. J. M. Normand, Nucl. Phys. A291, 126 (1977).
6. G. M. Hale and D. C. Dodder, LA-UR 80-1399 (1980) and Private Communication.
7. B. R. Leonard, Nuclear Cross Sections and Technology, NBS Special Publication 425, Vol. 1, 281 (1975).
8. H. D. Lemmel, ibid, Vol.1, 286 (1975).
9. L. Koester, W. Nistler, and W. Waschkowski, Phys. Rev. Letters 36, 1021 (1976).
10. L. Koester, In Springer Tracts in Modern Phys., Vol. 80, 1 (1977).
11. S. F. Mughabghab, The Third Neutron Cross Sections and Technology Conference Vol. 1, 386 (March 15-17, 1971).
12. A. M. Lane, Rev. Mod. Phys. 32 519 (1960).
13. J. W. Meadows and J. F. Whalen, Nucl. Sci. and Eng. 41 351 (1970).
14. S. E. Darden, et al., Nucl. Phys. A208, 77 (1973).
15. A. M. Lane and J. E. Lynn, Nucl. Phys. 17, 563, 586 (1961).
16. L. V. Groshev et al. Second Geneva Conf. of the Peaceful Uses of Atomic Energy, Vol. 15, 138 (1958).
17. O. A. Wasson, K. J. Wetzel, and C. K. Bocklemann, Phys. Rev. 136B, 1640, (1964).
18. L. B. Hughes, T. J. Kennett, and W. V. Prestwich, Nucl. Phys. 80, 131 (1966).
19. H. Gruppelaar, A. M. F. Den Kamp, and A. M. J. Spits, Nucl. Phys. A131, 180 (1969).
20. H, Gruppelaar, P. Spilling, A. M. J. Spits Nucl. Phys. 114A, 463 (1962).
21. S. E. Arnell, R. Hardell, O. Skeppstedt, and E.Wallander, Neutron Capture Gamma Ray Spectroscopy, Studsvik, August 1969, p. 231.
22. M. A. J. Mariscotti, J. A. Moragus, W. Gelletly, and W. R. Kane, Phys. Rev. Letters 22, 303 (1969).
23. A. M. J. Spits and J. A. Akkermans, Nucl. Structure Study with Neutrons, Budapest 1972. See also Nucl. Phys. 215A, 260 (1973).
24. L. M. Bollinger, Photonuclear Reactions and Applications, edited by B. Berman, Vol. 2, p. 783, March 26-30, 1973.
25. J. Kopecky, A. M. J. Spits and A. M. Lane, Phys. Letters 49B, 323 (1974).
26. S. F. Mughabghab, III School on Neutron Physics, Alushta, U.S.S.R., April 19-30 1978, p. 328.

27. S. F. Mughabghab, Phys. Letters 81B, 93 (1979). See also S. F. Mughabghab and R. E. Chrien, Neutron Capture Gamma Ray Spectroscopy edited by R. E. Chrien and W. R. Kane p. 265, Plenum Press New York and London 1979.
28. S. F. Mughabghab and D. I. Garber, BNL Report 325, Vol. I, Neutron Cross Sections.
29. S. G. Prussin et al., Phys. Rev. C16, 1991 (1977).
30. B. Fogelberg and W. Mampe, Z. Phys. A281, 89 (1977).
31. S. F. Mughabghab, Colloquium, Chalk River Nuclear Laboratory, Canada, August 21, 1980.
32. E. Jurney, Private Communication (1980).
33. M. A. Lone, Private Communication (1980).
34. H. Glattli et al., Le Journal De Physique 40, (1979) and references therein.
35. L. Koester, K. Knopf, and W. Waschowski, Z. Phys. A292, 95 (1979).
36. R. N. Glover and A. D. W. Jones, Nucl. Phys. 84, 673 (1966).
37. S. K. Datta, G. P. A. Berg, and P. A. Quin, Nucl. Phys. A 132, 1 (1978).
38. R. O. Lane, H. D. Knox, P. Hoffmann-Pinther, R. M. White, and G. F. Auchampaugh to be published Nucl. Phys.
39. B. A. Watson, P. P. Singh, and R. E. Segel, Phys. Rev. 182, 977 (1969).
40. L. Koester and K. Knopf, NEANDC(E)182U, Vol. 5, 78 (1978) and Private Communication (1980).
41. B. M. Craven and T. M. Sabine, Acta Cryst. 20, 214 (1966).
42. R. M. White, R. O. Lane, H. D. Knox, and J. M. Cox, and Nucl. Phys. A340, 13 (1980).
43. J. E. Monahan, H. T. Fortune, and C. M. Vincent, Phys. Rev. 3C, 2192 (1971).
44. Hans-Ulrich Gersch, Fortschritte der Physik, 17, 313 (1969).
45. S. Cohen and D. Kurath, Nucl. Phys. A101, 1 (1967).
46. C. H. Johnson, J. A. Harvey, D. C. Larson, and N. W. Hill, ORNL 5025 116 (1975).
47. A. Abragam et al., Phys. Rev. Letters 28, 805 (1972). See also Ref. 34.
48. A. D. Gul'ko, S. S. Trostin, and A. Hudoklin, Yad. Fiz. 6, 657 (1967).
49. P. Spilling, H. Gruppelaar, H. F. Devries, and A. M. J. Spits, Nucl. Phys. A111, 395 (1968).
50. A. A. Rollefson, P. F. Jones, and R. J. Shea, Phys. Rev. 1C, 1761 (1970).
51. C. A. Moseley and H. T. Fortune, Phys. Rev. 16C, 1697 (1977).
52. F. Ajzenberg-Selove, Nucl. Phys. A190, 1 (1972).
53. S. F. Mughabghab, Neutron Capture Gamma Ray Spectroscopy, Petten, the Netherlands, Sept. 2-6, 1974, p. 53.
54. P. M. Endt and C. Van der Leun, Nucl. Phys. A130, 1 (1978).
55. G. Brown, A. Denning, and J. G. B. Haigh, Nucl. Phys. A225, 267 (1974).

56. S. F. Mughabghab, Proceedings of the Specialists' Meeting on Neutron Cross Sections of Fission Product Nuclei, Bologna, Dec. 12-14 1979, NEANDC(E)209 "L", p. 1979.